INAF-Osservatorio astronomico di Torino
Technical Report nr.146

Spectral lines intensities (HI and OVI) measured by SOHO/UVCS

Silvio Giordano

Pino Torinese, 18 febbraio 2011

HI and OVI Spectral Lines Intensity measured by SOHO/UVCS

Silvio Giordano – February 18, 2011 - `UVCS_intensities.tex`

INAF/Osservatorio Astronomico di Torino

Contents

1. Abstract

The purpose of this document is to provide an average estimation of the measured intensities of the coronal spectral lines observed by UVCS/SOHO for different coronal structures and different periods of the solar cycle activity. The spectral lines analyzed are the HI Lyα, HI Lyβ, OVI 1032 and OVI 1038. We use a sample of UVCS observations performed during the solar minimum (1996/1997) and the solar maximum (1999/2000) to evaluated the intensities in two different coronal structures, that is the bright coronal streamers, and the dark polar coronal holes from the lower observed distances, $\sim$1.5 $R_\odot$ to $\sim$3.5 $R_\odot$. We find analytical formulas to describe the intensity profiles as a function of heliocentric distances for the different structures and solar cycle phases. Moreover, we provide an evaluation of the measured line widths of the coronal HI Lyα and OVI 1032 spectral lines for different coronal structures, at the solar minimum (1996). The code to plot the intensities as function of distance is *intensities_plot.pro in $HOME/PRO/UVCS_INTENSITY/* directory.

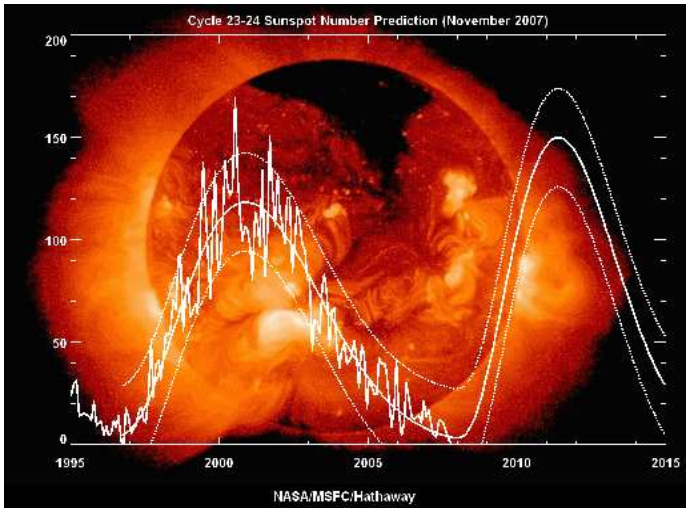

Fig. 1.— Sunspot cycle in the period of interest of UVCS observations.

2. HI Lyα

2.1. HI Lyα at Solar Minimum

As shown by the Sunspot cycle plots we can get the first year of the UVCS observations (1996) as sample of the Solar Minimum (Sunspot cycle plots shown in Figure 1 are available at `http://solarscience.msfc.nasa.gov/images/ssn_predict_l.gif`.

2.1.1. Observations

The streamers are identified as the bright structures extending along the radial direction in the equatorial region, for each mirror position we integrated approximately 140" along the slit around the maximum of the line intensity. The polar coronal holes intensities are those measured along the North or South radial polar axis integrated over 140" along the slit, except for the observation performed on Aug 29, 1996 where the roll angle is 195° because in that region there was a dark coronal hole. The observations used for streamers and CH are reported in Tables 1 and 2.

To verify the goodness of choice of streamers and CH we can build (or get from the web) the UVCS Lyα or LASCO/C2 WL synoptic images for each observation day. For streamer observations the available synoptic images from the observation days analyzed are here presented, see figures 2 to 4. In the case of polar coronal holes, in general during the solar minimum all the observations along the polar axis are representative of coronal hole behavior.

Table 1: Streamer Observations

FITS Files	PA (deg)
q96.04.11.00:59:53.lya.dat	270
q96.06.04.15:04:13.lya.dat	90
q96.08.31.16:58:37.lya.dat	255
q97.05.05.18:29:37.lya.dat	72

Table 2: Polar Coronal Hole Observations

FITS Files	PA (deg)
p96.04.06.07:21:14.lya.dat	360
q96.05.16.16:56:32.lya.dat	360
q96.05.21.00:35:10.lya.dat	360
d96.08.29.15:06:09.lya.dat	195
q97.05.03.18:46:34.lya.dat	360
q97.05.09.16:01:20.lya.dat	180
q97.12.20.13:16:25.lya.dat	180

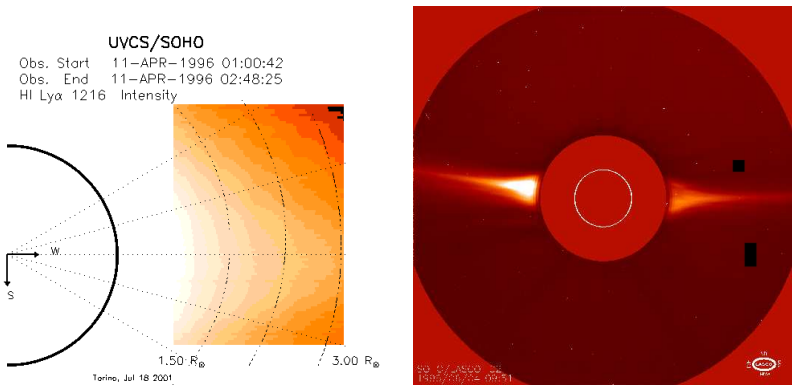

Fig. 2.— Left: UVCS HI Lyα intensity image of equatorial streamer observed in April 11, 1996, the maximum intensity of HI Lyα line is around the equatorial axis (270°). Right: LASCO/C2 White Light image of June 04, 1996, in this case in the FOV of UVCS the maximum intensity of HI Lyα line is around 85° (where LASCO shows a bright streamer).

2.1.2. Data Calibration

We use the HI Lyα primary channel of UVCS. To perform the calibrations we use the UVCS Torino Data Analysis Software ((DAS) Version 43 (*dpsto_43.pro*). The calibration file *D1.30.97.03.07.001* is used for the instrumental configuration, the parameters defined in this file are also used for radiometric calibration. For wavelength calibration and definition of instrumental line profile parameters we use the file *to.ins_cal.00.06.15*. The stray light (SL) and Interplanetary HI Lyα (IP) are subtracted by using the parameters of the file *to.str_cal.00.06.15.GS3* for all observations, except the file *to.str_cal.00.06.15.GS5* for those taken in May 1997 (because for that period we have CIII line and disk intensity observations). The HI Lyα disk intensity is from SOLSTICE data. Note the the instrumental profile used is a lorentzian function with 3 pixels full width. The DAS version used for the analysis of the data at the solar minimum is not the most recent, anyway we verified that the results are in good agreement with those obtained with the DAS Version 40 released on June 2006.

2.1.3. Analysis of Streamers Data

After the calibration, we rebin along the slit in order to obtain spatial elements of about 140", (total bin(s) = total FOV / 140), then we fit the spectra with a single gaussian function convolved with

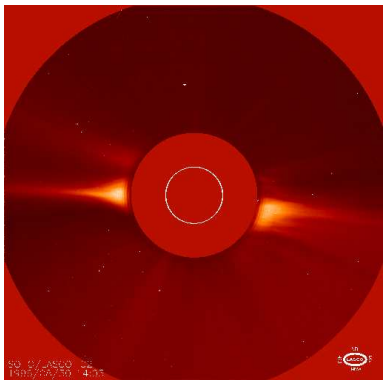

Fig. 3.— LASCO/C2 White Light image of August 30, 1996. in the FOV of UVCS the maximum intensity of HI Lyα line is between 253 to 268 degrees (where the WL streamers observed by LASCO seems less intense that the East limb streamer).

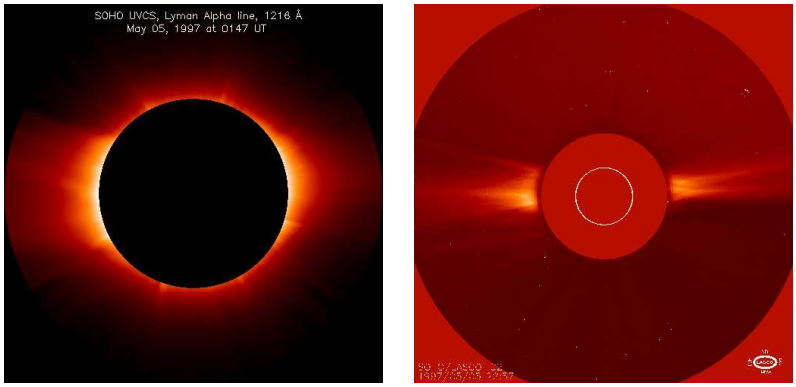

Fig. 4.— Synoptic images of May 5, 1997. Left: UVCS HI Lyα. Right: LASCO/C2 White Light. In the FOV of UVCS the maximum intensity of HI Lyα line is between 80 to 95 degrees.

the instrumental profile and we select, for every mirror position, the position along the slit where there is a maximum of the intensity A example of line fitting is reported in the Figure 6.

For the observation performed on Apr 11, 1996 we verify the influence of stray light and IP corrections on the line intensity by fitting the spectra before the stray light subtraction. In the case of streamers the correction is almost negligible because is the order of few percent, as shown in Table 12

Table 3: Stray Light and Interplanetary HI Lyα in a Coronal Streamer

Helioc. distance	SL and IP
1.51	3.1%
1.71	1.5%
1.91	0.7%
2.21	0.5%
2.61	0.5%
3.01	0.6%

The intensity results for the analyzed streamers are reported in Figure 6. We can note that the statistical error bars are smaller than the variation of intensity for different observation days. The numerical values are in Table 13.

The average radial dependence of the **HI Lyα** intensity in coronal **streamers** at solar **minimum**

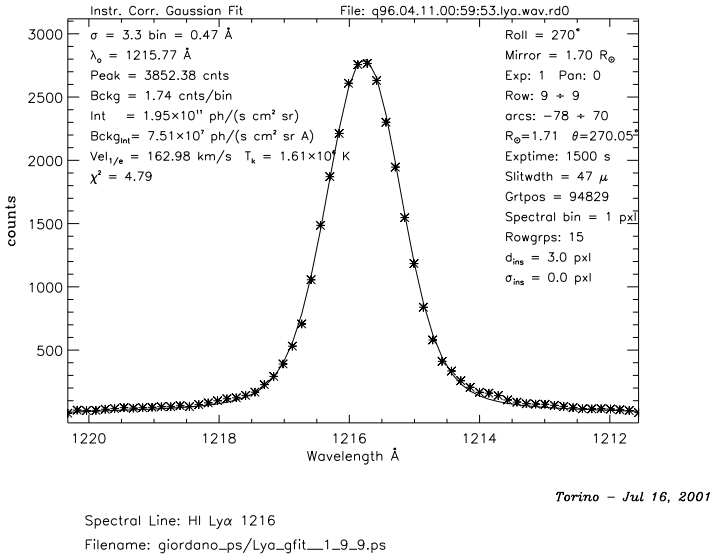

Fig. 5.— Example of HI Lyα spectral line fitting.

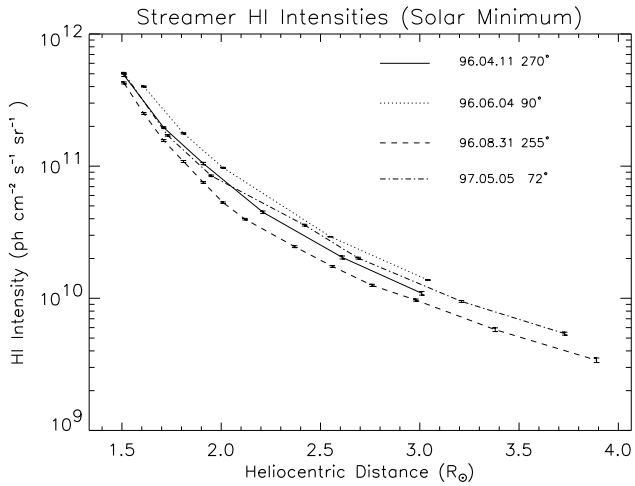

Fig. 6.— HI Lyα intensity as a function of heliocentric distance for different observed streamers

is obtained by fitting the data with a power law:

$$I \;=\; c \times \left[a_1 \times \left(\frac{r}{R_\odot}\right)^{b_1} + a_2 \times \left(\frac{r}{R_\odot}\right)^{b_2} + a_3 \times \left(\frac{r}{R_\odot}\right)^{b_3} \right] \qquad (1)$$

with the following parameters:
$a_1 = 518.56$, $a_2 = 32.17$, $a_3 = 1.29$, $b_1 = -11.07$, $b_2 = -5.10$, $b_3 = -2.32$, $c = 4.85\times\ 10^{10}$
((see program *str_int_report.pro* in $*HOME/PRO/UVCS_INTENSITY/* .

2.1.4. Analysis of Coronal Holes Data

As for streamer data, after the calibration, we rebin the data along the slit in order to obtain spatial elements of about 140 arcseconds, then we fit the spectra with a single gaussian function and we select, for every mirror position, the center of the FOV along the slit, which is the axis of the polar coronal hole when the instrument roll is oriented to North or South Pole. In Figure 7 we report the intensity profiles as a function of heliocentric distance for the different analyzed coronal holes. The numerical values of

HI Lyα intensity observed in polar coronal hole are in Table 13. As reported in Table 13, we note that the higher values are fund for observation of Aug 29, 1996, when the axis of the observation was 195°, therefore this observation could be not representative of coronal hole and so it is not plotted in Figure 7.

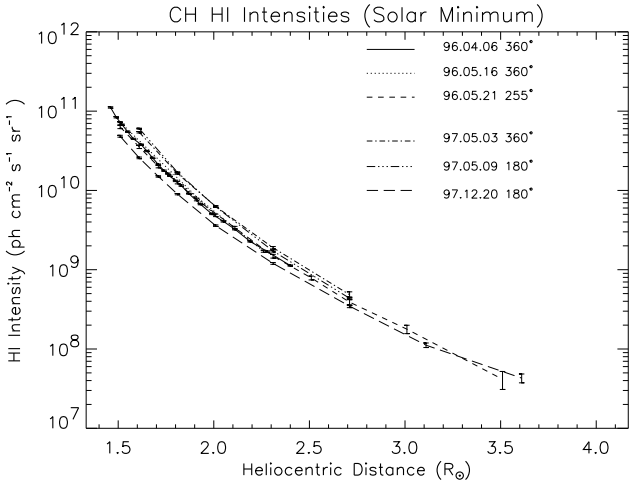

Fig. 7.— HI Lyα intensity as a function of heliocentric distance for different observed polar coronal holes

Table 4: Stray Light in a Coronal Hole

Helioc. distance	SL and IP
1.51	33%
1.61	25%
1.71	20%
1.81	16%
2.01	13%
2.31	14%
2.71	24%
3.11	57%

As for the streamers we can describe the average radial dependence of the **HI Lyα** intensity in **coronal holes** at solar **minimum** by a power law, in this case we obtain the best fit by using the following parameterization:

$$I \;=\; c \times \left[a_1 \times \left(\frac{r}{R_\odot} \right)^{b_1} + a_2 \times \left(\frac{r}{R_\odot} \right)^{b_2} \right] \tag{2}$$

with the parameters: $a_1 = 2155.27$, $a_2 = 128.98$, $b_1 = -10.77$, $b_2 = -6.73$, $c = 2.04\times\ 10^9$
((see program *ch_int_report.pro* in $*HOME/PRO/UVCS_INTENSITY/*.

We verify the influence of stray light and IP correction for coronal hole observations by comparing the intensity obtained before and after that subtraction for the observation performed on Dec 20, 1997, which represent the worst case because the low intensity (see Figure 7). The stray light percent are reported at different height in Table 4. We note that in this low intensity region the stray light contribution is not negligible and the intensity subtracted increases at higher heights because of the IP HI Lyα contribution, which is expected $\simeq\ 4 \times 10^7\ ph\ cm^{-2}\ s^{-1}\ sr^{-1}$.

In fact, as shown in Table 13, for Dec 20, 1997 observation at distance greater than 3.61 $R_\odot$ the observed intensity is of the same order of magnitude as the IP emission, therefore a careful analysis could be necessary to analyze the HI Lyα line in low emission CH.

2.1.5. Streamers and Coronal Holes Comparison

In Figure 8 we show the HI Lyα intensity comparison between coronal streamers and coronal holes, for both structures the bands represent the variation of intensity from different observations and the curves between the higher and lower values are the results of parameterization given by equations 1 and 2.

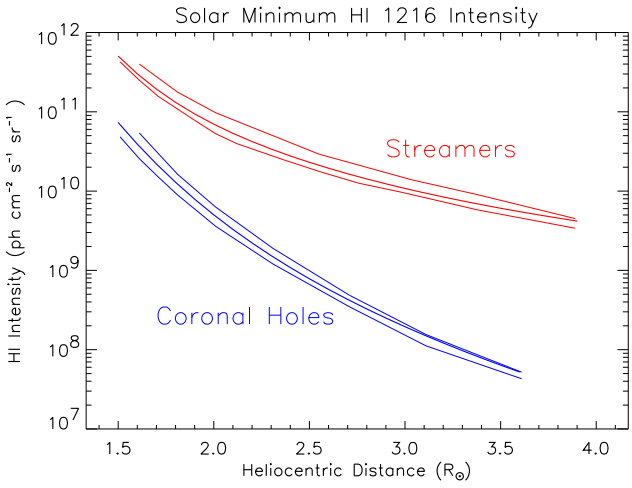

Fig. 8.— HI Lyα intensity as a function of heliocentric distance at the Solar Minimum (1996/19997) for equatorial streamers and polar coronal holes.

2.2. HI Lyα at Solar Maximum

The Maximum of the Solar Activity in the cycle 23 was during the year 2000. Since the beginning of the year 2000 we stop the regular observations height 1.5 $R_\odot$ so the lower observations are at 1.6 $R_\odot$ and the HI Lyα is detected by the Redundant Channel. At solar maximum it is more difficult identify the streamer and hole structures, then we use the Carrington maps (See Figure 9) of the intensity to find the bright (streamers) and faint structures (coronal holes).

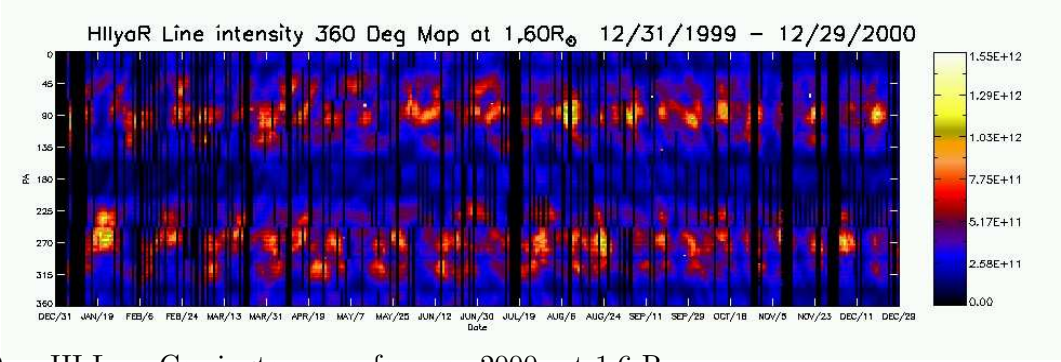

Fig. 9.— HI Lyα Carrington map for year 2000. at 1.6 $R_\odot$.

2.2.1. Observations

The observations used for equatorial and polar regions study during the solar maximum are reported in Table 5 and 6.

Table 5: Equatorial Observations

FITS Files	PA (deg)
s00.08.08.05:31:02.ovi.dat	90 use this only at leas for HI Lyα
s00.01.21.00:47:30.ovi.dat	270 too faint !
00.10.01.???	90
00.12.20.???	90
00.08.24.???	270
00.12.06.???	270

Table 6: Polar Observations

FITS Files	PA (deg)
d00.03.19.18:05:59.ovi.dat	360
d00.11.22.08:21:47.ovi.dat	180

2.2.2. Data Calibration and Analysis

We use the HI Lyα redundant channel of UVCS. To perform the calibrations we use the UVCS Data Analysis Software (DAS) Version 40 with the features included into the Torino version (see prf 2.2). For the equatorial data we work as for the streamer data at the solar minimum; after the calibration, we rebin the data along the slit in order to obtain spatial elements of about 140", then we fit the spectra and we select the position along the slit where there is a maximum of the intensity. For polar data, as for coronal hole data at solar minimum, we select the center of the FOV along the slit.

The average radial dependence of the **HI Lyα** intensity at solar **maximum** is defined by the equation 1 power law fit: where for the **equatorial region** the parameters are:
$a_1 = 3.80972$,, $a_2 = 0.442793$, $a_3 = 0.534379$, $b_1 = -11.7479$, $b_2 = -4.87657$, $b_3 = -5.92358$, $c = 1.6436 \times 10^{13}$

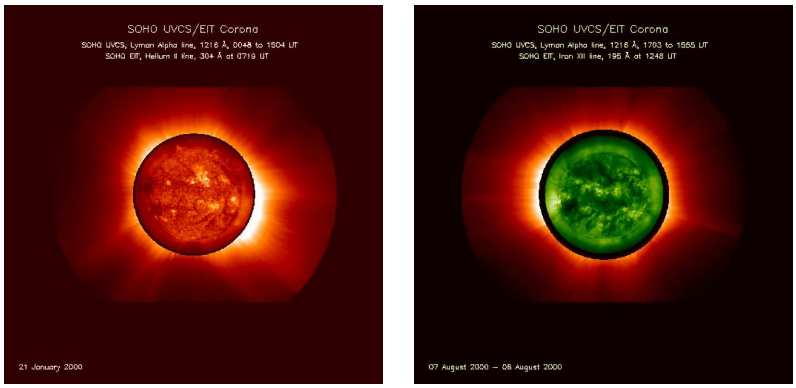

Fig. 10.— Left: UVCS HI Lyα and EIT HeII intensity image observed in Jan 21, 2000. Right: UVCS HI Lyα and EIT HeII intensity image observed in Aug 07, 2000. These days have been used to evaluate the intensity in the equatorial regions.

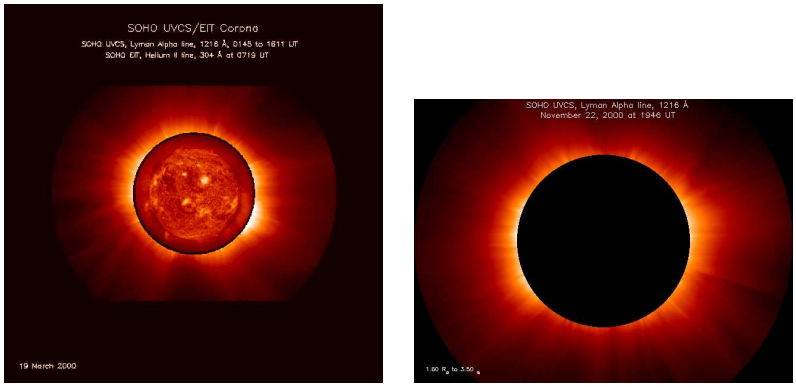

Fig. 11.— Left: UVCS HI Lyα and EIT HeII intensity image observed in Mar 19, 2000. Right: UVCS HI Lyα intensity image observed inNov 22, 2000. These days have been used to evaluate the intensity in the polar regions

while for the **polar region** are:
$a_1 = 3194.05$, $a_2 = 262.171$, $a_2 = 0.0$, $b_1 = -7.99648$, $b_2 = -3.92075$, $b_2 = 1.$, $c = 2.63\times\ 10^9$
((see program *int_report_max.pro* in $*HOME/PRO/UVCS_INTENSITY/* .

2.2.3. Equatorial and Polar Intensity Comparison

In Figure 12 we show the HI Lyα intensity comparison between equatorial and polar regions observed at the time of Solar Maximum. The bands represent the variation of intensity from different observations and the curves between the higher and lower values are the results of parameterization given by Equations 3 and 4.

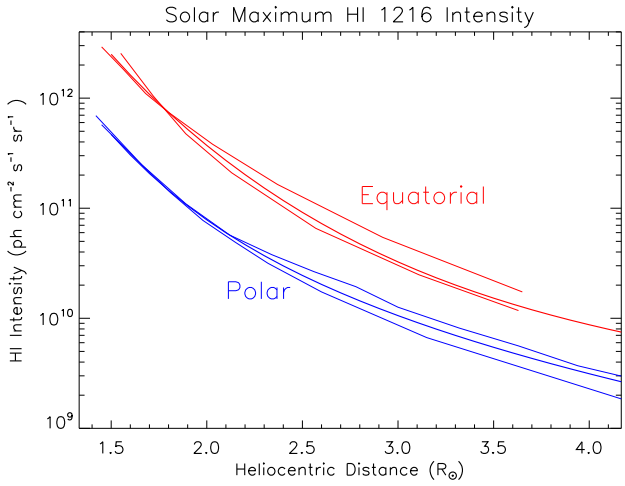

Fig. 12.— HI Lyα intensity as a function of heliocentric distance at the Solar Maximum (2000) for equatorial and polar regions.

3. OVI 1032

3.1. OVI 1032 at Solar Minimum

We analyze the same observations used to study the HI Lyα intensity at the solar minimum, see section 2.1.

3.1.1. Observations

The observations used and the relative FITS files are described in Section 2.1, here in Table 7 we report the FITS list, the question mark means that those files have not analyzed yet.

Table 7: Streamer Observations

FITS Files	PA (deg)
q96.04.11.00:59:53.ovi.dat	270
q96.06.04.15:04:13.ovi.dat	90
q96.08.31.16:58:37.ovi.dat	255
q97.05.05.18:29:37.ovi.dat	72

Table 8: Polar Coronal Hole Observations

FITS Files	PA (deg)
p96.04.06.07:21:14.ovi.dat	360
q96.05.16.16:56:32.ovi.dat	360
q96.05.21.00:35:10.ovi.dat	360 (jop2)
q97.05.03.18:46:34.ovi.dat	360

3.1.2. Data Calibration

The data are, obviously, from the OVI channel of UVCS. To perform the calibrations we use the UVCS Torino Data Analysis Software ((DAS) Version 40_sg0.0. Wavelength calibration, instrumental line profile and stray light (SL) are taken into account in the same way as described in Section 2.2. The OVI 1032 disk intensity is from UVCS observation performed on Dec 8, 1997. Note the the instrumental profile used is a lorentzian function with 1.2 pixels full width.

3.1.3. Analysis of Streamers Data

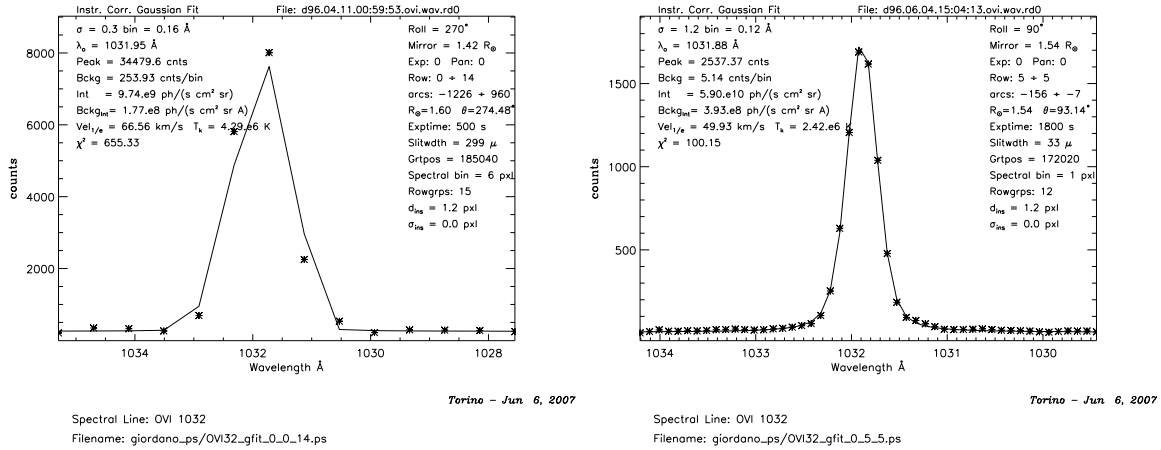

Fig. 13.— OVI 1032 spectral line fitting examples. Left: slit = 300 μn. Right: slit = 33 μn

We sum together all the exposures with the same mirror position. Then after the calibration, we select the OVI 1032 wavelength range, we rebin the data along the slit in order to obtain spatial elements of about 140", (total bin(s) = total FOV / 140), we compute the radiometric factor and finally we fit the spectra with a single gaussian function convolved with the instrumental profile and we select, for every mirror position, the position along the slit where there is a maximum of the intensity. A couple of examples of line fitting are in Figure 13.

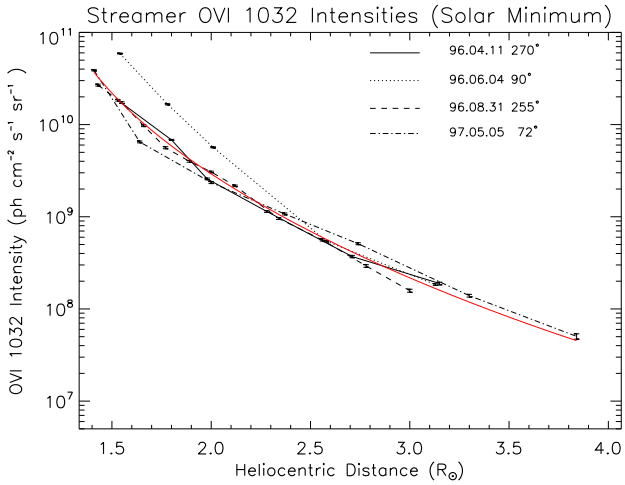

Fig. 14.— OVI 1032 intensity as a function of heliocentric distance for different streamers

The intensity profiles for the analyzed streamers are in Figure 14. We can note that the statistical error bars are smaller than the variation of intensity for different observations. The numerical values are in Table 14. The average radial profile of **OVI 1032** intensity in coronal **streamer** at solar **minimum** is given by the power law:

$$I \;=\; c \times \left[a_1 \times \left(\frac{r}{R_\odot}\right)^{b_1} + a_2 \times \left(\frac{r}{R_\odot}\right)^{b_2} + a_3 \times \left(\frac{r}{R_\odot}\right)^{b_3} \right] \tag{3}$$

with the following parameters:
$a_1 = 246.194$, $a_2 = 31.60$, $a_3 = 0.00890$, $b_1 = -15.02$, $b_2 = -6.36$, $b_3 = -5.96$, $c = 7.96\times\ 10^9$
((see program *ovi_str_int_report.pro* in *../PRO/UVCS_INTENSITY/* directory.

3.1.4. Analysis of Coronal Holes Data - work in progress

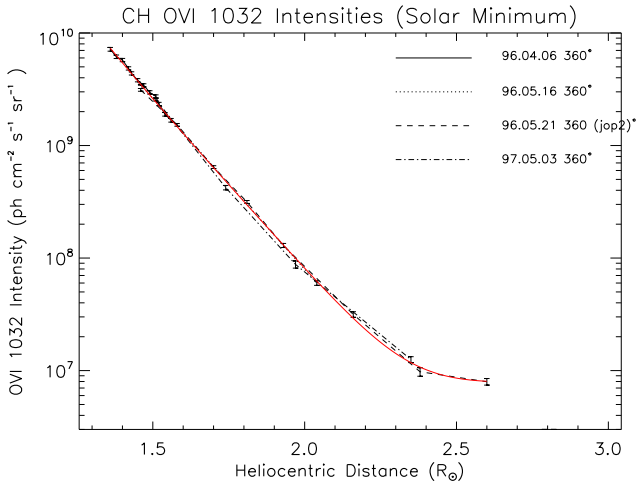

Fig. 15.— OVI 1032 intensity as a function of heliocentric distance for different observed polar coronal holes

See Section 2.4 The files ready for fitting are in the PRO/UVCS_INTENSITY/ directory with the extension *.rd0*, and the results of fitting in the image files *.ima*. The stray light is not subtracted therefore the values has to be considered as upper limit of the observed intensity. In Figure 15 we report the intensity profiles as a function of heliocentric distance for the different analyzed coronal holes. The numerical values of OVI 1032 intensity observed in polar coronal hole are in Table 14.

As for the streamers we can describe the radial dependence of the **OVI 1032** intensity in **coronal holes** with a power law given by equation 4 with the following parameters:
$a_1 = 116.34$, $a_2 = -68.95$, $a_3 = 5.472$, $b_1 = -8.1026$, $b_2 = -6.97$, $b_3 = -5.1262$, $c = 2.74 \times 10^9$
(see program *ovi_ch_int_report.pro* in $*HOME/PRO/UVCS_INTENSITY/*.

3.2. OVI 1032 at Solar Maximum

3.2.1. Streamer

Preliminarily, missing the subtraction of the stray light contribution we perform the OVI 1032 total intensity analysis of the first 2 streamers observations reported in Table 5. The analysis has been performed as for OVI 1032 spectral line, described in Section 3.1.3, that is, after the calibration, we rebin the data along the slit in order to obtain spatial elements of about 140", then we fit the spectra and we select the position along the slit where there is a maximum of the intensity.

The radial dependence of the **OVI 1032 streamer** intensity at solar **maximum** can be described by the equation 4 with the following parameters:
$a_1 = 4151.24$, $a_2 = 243.055$, $a_3 = 8.6228$, $b_1 = -9.4064$, $b_2 = -9.48425$, $b_3 = -4.426$, $c = 4.0372 \times 10^9$

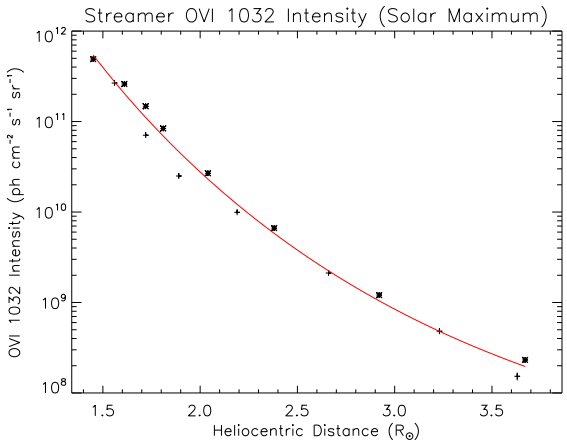

Fig. 16.— OVI 1032 intensity as a function of heliocentric distance for 2 streamers at Solar Maximum.

4. OVI 1037

4.1. OVI 1037 at Solar Minimum

4.1.1. Streamer

Preliminarily the intensity analysis has been performed for OVI 1037 data taken on My 05 1997 (FITS q97.05.05.18:29:37.ovi.dat). We do not subtract the stray light contribution.

The radial dependence of the **OVI 1037 streamer** intensity at solar **minimum** can be described by the equation 4 with the following parameters:
$a_1 = 2624.26$, $a_2 = 1.88626$, $a_3 = 0.39446$, $b_1 = -24.99$, $b_2 = -5.65$, $b_3 = -5.62$, $c = 1.76\times\ 10^{10}$

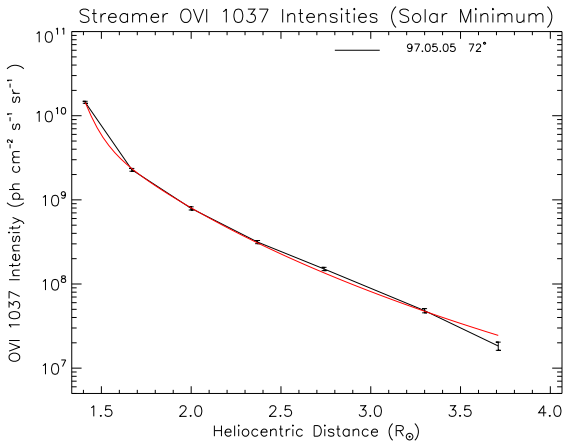

Fig. 17.— OVI 1037 intensity as a function of heliocentric distance for streamer observed on May 05, 1997.

4.2. OVI 1037 at Solar Maximum

4.2.1. Streamer

We perform the OVI 1037 total intensity analysis of the first 2 streamers observations reported in Table 5. The analysis has been performed as for OVI 1032 spectral line, described in Section 3.1.3,

The radial dependence of the **OVI 1037 streamer** intensity at solar **maximum** can be described by the equation 4 with the following parameters:
$a_1 = 1465.64$, $a_2 = -1013.3$, $a_3 = 62.307$, $b_1 = -8.54155$, $b_2 = -7.9448$, $b_3 = -6.3807$, $c = 1.606\times\ 10^{10}$

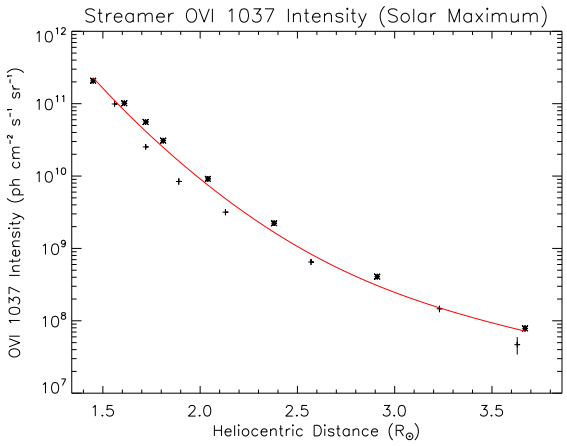

Fig. 18.— OVI 1037 intensity as a function of heliocentric distance for 2 streamers at Solar Maximum.

5. HI Lyβ

5.1. HI Lyβ at Solar Minimum

5.1.1. Streamer

Preliminarily, missing the subtraction of the stray light contribution we perform the HI Lyβ total intensity analysis of the 4 streamers observations reported in Table 7. The analysis has been performed as for OVI 1032 spectral line, described in Section 3.1.3, that is, after the calibration, we rebin the data along the slit in order to obtain spatial elements of about 140", then we fit the spectra and we select the position along the slit where there is a maximum of the intensity.

The radial dependence of the **HI Lyβ streamer** intensity at solar **minimum** can be described by the equation 4 with the following parameters:
$a_1 = 52.154$, $a_2 = 8.49924$, $a_3 = 0.1236$, $b_1 = -7.3408$, $b_2 = -6.1351$, $b_3 = -1.4091$, $c = 3.8120\times\ 10^8$

5.2. HI Lyβ at Solar Maximum

5.2.1. Streamer

Preliminarily, missing the subtraction of the stray light contribution we perform the HI Lyβ total intensity analysis of the first 2 streamers observations reported in Table 5. The analysis has been performed as described in previous Section.

The radial dependence of the **HI Lyβ streamer** intensity at solar **maximum** can be described by the equation 4 with the following parameters:
$a_1 = 1667.8$, $a_2 = 6.60137$, $a_3 = 0.216383$, $b_1 = -10.8224$, $b_2 = -4.71977$, $b_3 = -2.3993$, $c = 8.774\times\ 10^8$

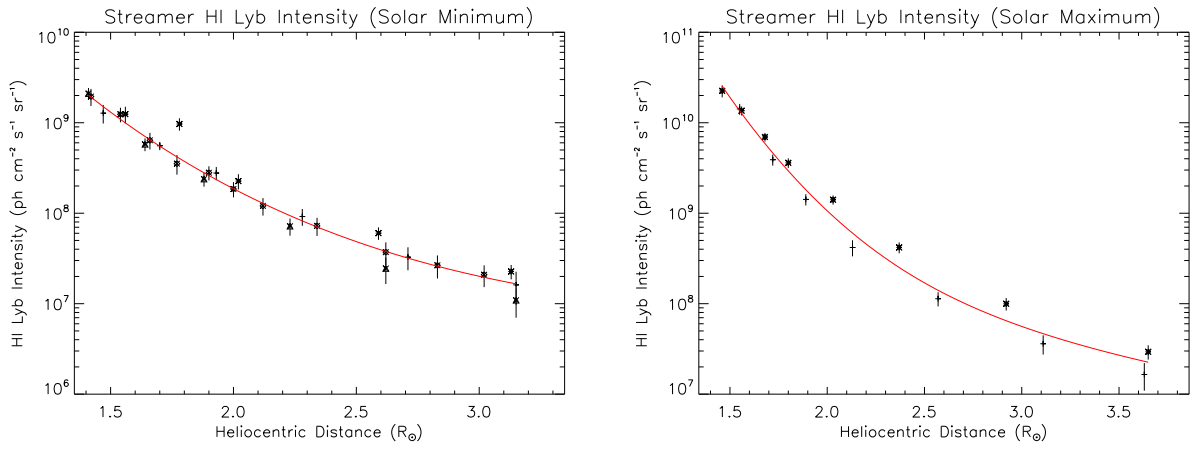

Fig. 19.— Left: HI Lyβ intensity as a function of heliocentric distance for 4 streamers at Solar Minimum(see Table 7). Right: for 2 streamers at Solar Maximum(see Table 5). These plot have been produced by *lyb_str_int_minmax_report.pro* in $*HOME/PRO/UVCS_INTENSITY/* directory.

6. HI and OVI spectral lines widths

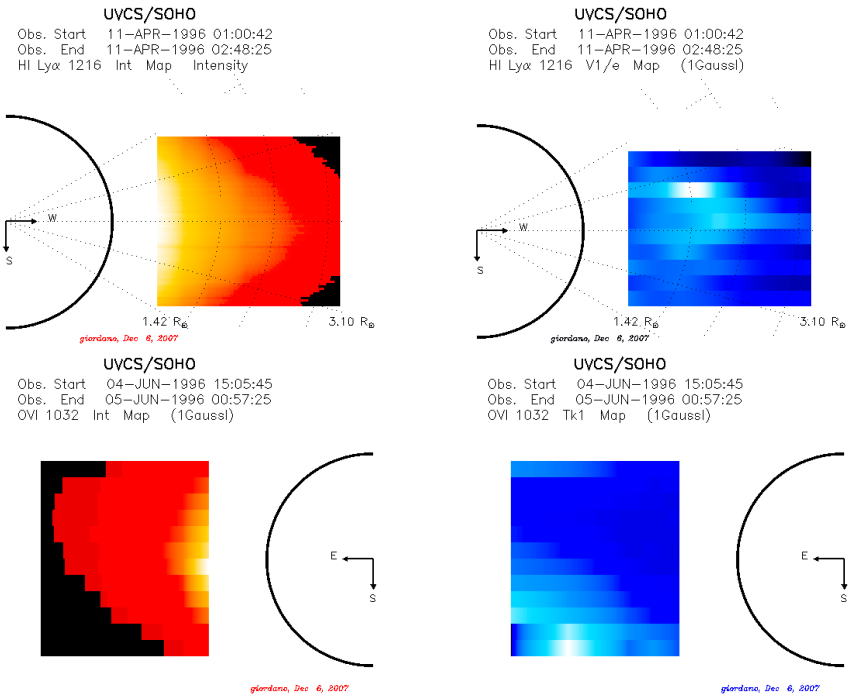

Fig. 20.— UVCS HI Lyα intensity (upper left) and $v_{1/e}$ (upper right) image of equatorial streamer observed in April 11, 1996. UVCS OVI 1032 intensity (lower left) and $v_{1/e}$ (lower right) image of equatorial streamer observed in June 4, 1996. In dark blue represents smaller line widths.

A sample of UVCS observations have been analyzed to provide an evaluation of the line widths of the coronal HI Lyα and OVI 1032 spectral lines observed by UVCS/SOHO for different coronal structures, (bright coronal streamers and dark polar coronal holes) from ~1.5 $R_\odot$ to ~3.5 $R_\odot$. at the solar minimum (1996).

6.1. Line widths in Coronal Streamers

Table 9: Streamer Observations used for line width study

FITS Files	PA (deg)	slit um	spectral binning [pxl]	grtpos
q96.04.11.00:59:53.lya.dat	270	47	1	94830
q96.06.04.15:04:13.lya.dat	90	49	1	104800
q96.06.04.15:04:13.ovi.dat	90	33	1	172000

We choose the equatorial observations summarized in the Table 1. For each mirror position we integrated approximately 140" along the slit and we get the intensity and width of the line at the center of the slit (that is the lower distance from Sun center).

The line widths are determined by fitting the spectra as described in the Appendix I. An evaluation of the stray light contribution on the line width and line intensity has been performed as showed in the Figure 8 (see also Section 2.3)

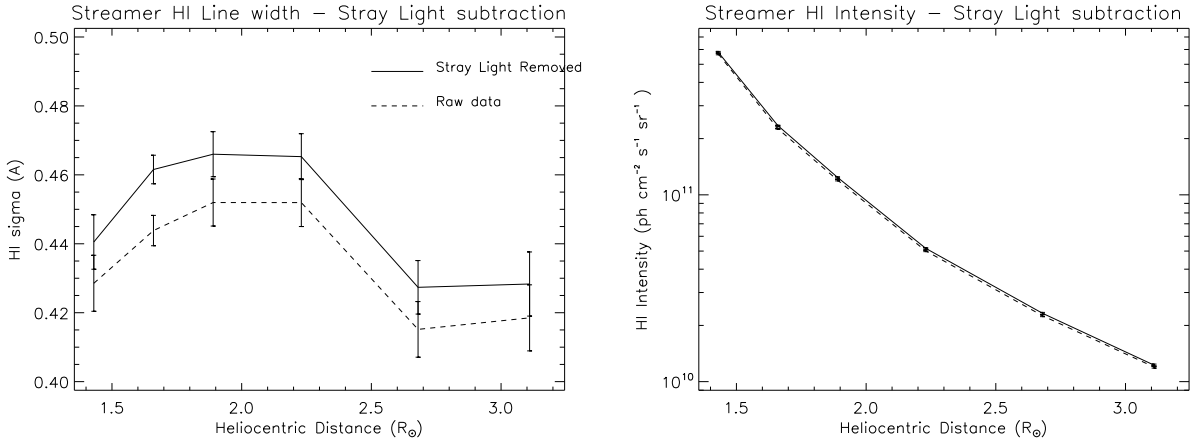

Fig. 21.— Stray light contribution on the HI Lyα line width (left) and on the line intensity (right)

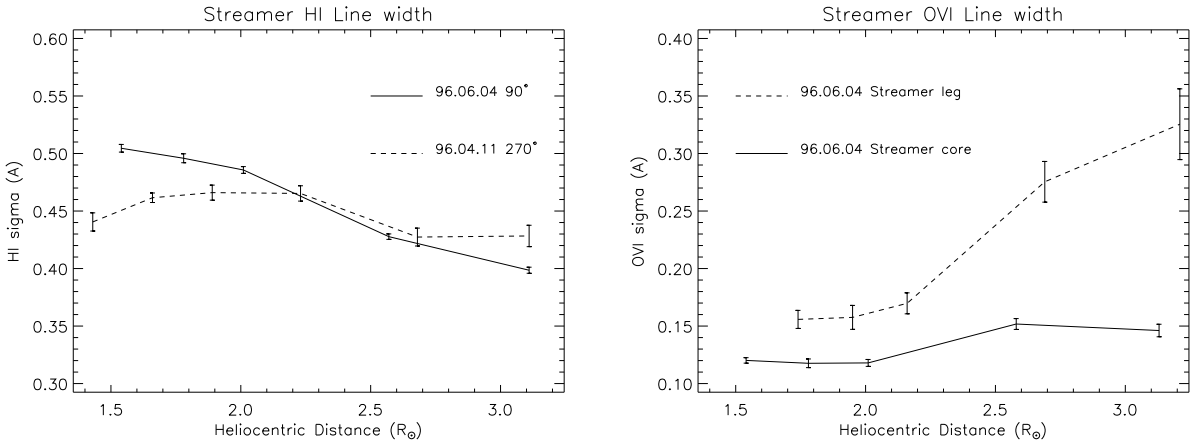

Fig. 22.— HI Lyα line width for two streamers (left) and OVI 1032 line width for the streamer core and streamer leg (right)

7. Appendix I: Fit of UVCS spectral data

To determine the parameters of the emitted spectral lines in a selected spatial regions, after the configuration and wavelength calibration, we compute the radiometric factor, R_{fact}, which allows the conversion of the counts into intensity units. The total line intensity is measured in *photons* cm^{-2} s^{-1} sr^{-1}, and R_{fact} is measured in *photons* cm^{-2} s^{-1} sr^{-1} $\AA^{-1}$. In this way we can apply the Poissonian statistics to compute the errors on the parameters obtained by the fitting procedure, finally by using the radiometric factor we convert the total counts into physical units. We fit the spectral profile from a single spatial detector bin or summed over the selected region along the slit, with a single Gaussian function, $G(\lambda)$, convolved with the spectral detector profile, $D(\lambda)$, and a rectangular slit width function, S, to take into account the instrumental contribution to the lines width, finally a constant background, *bck*, is added. Therefore the fitting function is:

$$F(\lambda) \;=\; \Big(G(\lambda) \;*\; D(\lambda) * S \Big) \;+ bck \tag{4}$$

where the physical parameters are defined by the free parameters of a Gaussian function:

$$G(\lambda) \;=\; G_0 \; exp\left[-\frac{1}{2} \left(\frac{\lambda - \lambda_0}{\sigma_\lambda} \right)^2 \right] \tag{5}$$

where $G_0 = G(\lambda_0)$ is the peak of the Gaussian function in *counts*, λ_0 is the line centroid in Å and σ_λ is the standard deviation in Å. From this function we derive the following parameters:

- "Most probable velocity" of the emitting atoms (or ions) in a Maxwellian velocity distribution which is given by the 1/e velocity, $v_{1/e}$, of a Gaussian velocity distribution along the line-of-sight (l.o.s.):

$$v_{1/e} \;=\; \sqrt{2} \frac{c}{\lambda_0} \sigma_\lambda \;\; [km\ s^{-1}] \tag{6}$$

  where $c = 2.9979 \;\times\; 10^5\ km\ s^{-1}$ is the speed of light and λ_0 is the wavelength at rest (for HI Lyα $\lambda_0 = 1215.67$ Å and for OVI 1032 $\lambda_0 = 1031.91$ Å. Therefore approximately we can use for HI: $v_{1/e} \;\simeq\; 349 \times \sigma_\lambda\ km\ s^{-1}$ and for OVI 1032: $v_{1/e} \;\simeq\; 411 \times \sigma_\lambda\ km\ s^{-1}$ where σ_λ is measured in Å).

- Kinetic temperature of the emitting ions along the l.o.s.:

$$T_k \;=\; \frac{A_i m_p}{2 k_B} v_{1/e}^2 \;\; [^\circ K] \tag{7}$$

  where A_i is the ion mass number, (A_i=1 for Hydrogen, A_i=16 for Oxygen), $m_p = 1.6725 \;\times\; 10^{-24}\ g$ is the proton mass and $k_B = 1.3807 \;\times\; 10^{-16}\ erg^\circ K^{-1}$ is the Boltzmann constant, (Approx. for HI atoms $T_k \;\simeq\; 60.6 \times v_{1/e}^2\ ^\circ K$ and for OVI ions $T_k \;\simeq\; 969 \times v_{1/e}^2\ ^\circ K$ where $v_{1/e}$ is in km s^{-1}).

- Spectral line intensity:

$$I \;=\; \sqrt{2\pi} \sigma_\lambda G_0 \frac{R_{fact}}{R_{corr}} \;\; [photons\ cm^{-2}\ s^{-1}\ sr^{-1}] \tag{8}$$

  where G_0 is the peak of the Gaussian function in *counts* and R_{corr} is the number of the combined spatial bins.

- "Total counts" detected by the instrument:

$$C_{tot} \;=\; \sum_{i=0}^{N} (c_i - bck) \tag{9}$$

  where c_i are the counts at each spectral bin, N is the number of bins in the spectral window and *bck* in the background in *counts/bin* from the fitting function.

- The width of a gaussian function should be also characterized by the Full Width at Half Maximum (FWHM), or by the Half Width at $1/e$ (g), the relations between these quantities and the standard deviation σ_λ are:

$$FWHM = 2\sqrt{2 \log 2}\, \sigma_\lambda \simeq 2.35\, \sigma_\lambda,$$
$$g = \sqrt{2}\, \sigma_\lambda \simeq 1.41\, \sigma_\lambda.$$

8. Appendix II: Coronal Intensity Profiles Fitting Parameters

$$I = c \times \left[a_1 \times \left(\frac{r}{R_\odot} \right)^{b_1} + a_2 \times \left(\frac{r}{R_\odot} \right)^{b_2} + a_3 \times \left(\frac{r}{R_\odot} \right)^{b_3} \right] \quad (10)$$

Table 10: Fitting coefficients

Spectral Line	Structure	Cycle Phase	c $\times 10^8$	a_1	a_2	a_3	b_1	b_2	b_3
HI Lyα	CS	Minimum	485	518.56	32.17	1.29	-11.07	-5.10	-2.32
HI Lyα	Equat	Maximum	164360	3.80972	0.442793	0.534379	-11.7479	-4.87657	-5.92358
HI Lyβ	CS	Minimum	3.8120	52.154	8.49924	0.1236	-7.3408	-6.1351	-1.4091
HI Lyβ	Equat	Maximum	8.774	1667.8	6.60137	0.216383	-10.8224	-4.71977	-2.3993
OVI 1032	CS	Minimum	79.6	246.194	31.60	0.00890	-15.02	-6.36	-5.96
OVI 1032	Equat	Maximum	40.372	4151.24	243.055	8.6228	-9.4064	-9.48425	-4.426
OVI 1037	CS	Minimum	176	2624.26	1.88626	0.39446	-24.99	-5.65	-5.62
OVI 1037	Equat	Maximum	160.6	1465.64	-1013.3	62.307	-8.54155	-7.9448	-6.3807
HI Lyα	CH	Minimum	20.4	2155.27	128.98		-10.77	-6.73	
HI Lyα	Polar	Maximum	26.3	3194.05	262.171		-7.99648	-3.92075	
HI Lyβ	CH	Minimum							
HI Lyβ	Polar	Maximum							
OVI 1032	CH	Minimum	27.4	116.34	-68.95	5.472	-8.1026	-6.97	-5.1262
OVI 1032	Polar	Maximum							
OVI 1037	CH	Minimum							
OVI 1037	Polar	Maximum							

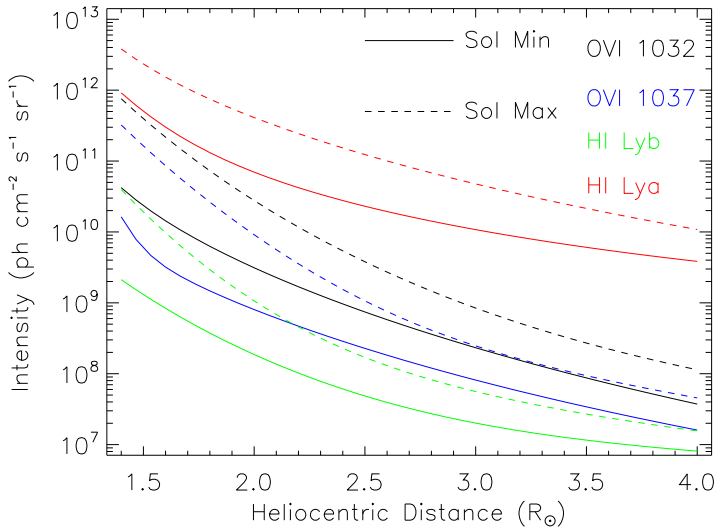

Fig. 23.— Coronal Intensity as function of heliocentric distance for main observed spectral lines in coronal streamers. (Output from *intensities_plot.pro* in $*HOME/PRO/UVCS_INTENSITY/*).

9. Appendix III: Down lo Disk Intensity Profiles Fitting Parameters

$$I = c \times \left[a_1 \times \left(\frac{r}{R_\odot} \right)^{b_1} + a_2 \times \left(\frac{r}{R_\odot} \right)^{b_2} + a_3 \times \left(\frac{r}{R_\odot} \right)^{b_3} \right] \quad (11)$$

Table 11: Fitting coefficients modified to get the disk intensities

Spectral Line	Structure	Cycle Phase	c $\times 10^9$	a_1	a_2	a_3	b_1	b_2	b_3
HI Lyα	CS	Minimum	426.527	10480.8	2.94073	66.4082	-37.7416	-4.02709	-12.1995
HI Lyα	Equat	Maximum	60326.1	63.3883	-63.094	130.660	-5.41252	-5.41262	-25.4170
HI Lyβ	CS	Minimum	5.59483	7074.86	3.49756	0.00167984	-36.3908	-6.76766	-0.09890
HI Lyβ	Equat	Maximum	6.50203	10053.7	219.495	0.518230	-84.3422	-10.7309	-3.91743
OVI 1032	CS	Minimum	57.6317	534.643	5.28221	-0.679059	-23.6087	-6.48423	-6.49250
OVI 1032	Equat	Maximum	10.4809	1722.06	3615.18	5.55364	-9.46485	-54.9453	-4.80038
OVI 1037	CS	Minimum	15.0185	896.169	136.831	2.54935	-21.7629	-21.7564	-5.60141
OVI 1037	Equat	Maximum	9.68650	1844.19	1045.92	0.512518	-37.0579	-10.1873	-3.49629

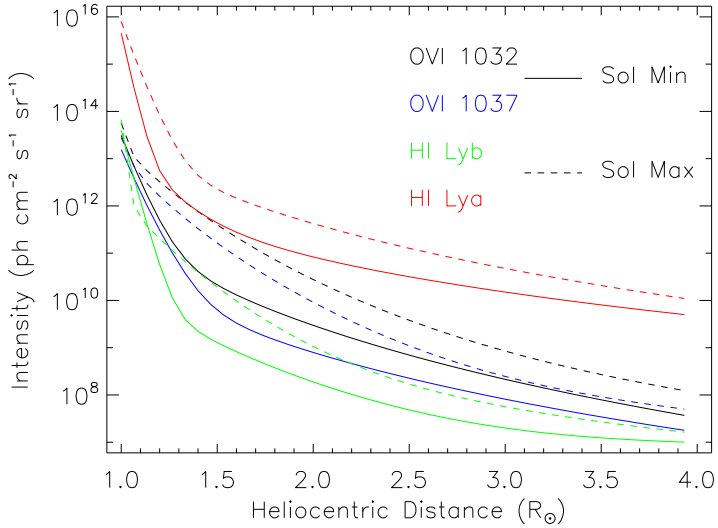

Fig. 24.— Intensity as function of heliocentric distance for main observed spectral lines in coronal streamers, the heights are down to solar disk. (Output from *intensities_plot_disk.pro* in $*HOME/PRO/UVCS_INTENSITY/*).

10. Appendix IV: HI Lyα and OVI 1032 Intensities ... numbers

Table 12: Streamer HI Lyα Intensities at the Solar Minimum (see Figure 6)

Date	Distance ($R_\odot$)	PA (deg)	Intensity ($ph\ cm^{-2}\ s^{-1}\ sr^{-1}$)
96.04.11	1.51	267	4.89×10^{11}
	1.71	268	1.96×10^{11}
	1.91	268	1.05×10^{11}
	2.21	268	4.48×10^{10}
	2.61	268	2.04×10^{10}
	3.01	269	1.09×10^{10}
96.06.04	1.61	84	4.01×10^{11}
	1.81	85	1.77×10^{11}
	2.01	86	9.72×10^{10}
	2.55	80	2.92×10^{10}
	3.04	81	1.38×10^{10}
96.08.31	1.51	253	4.26×10^{11}
	1.61	258	2.50×10^{11}
	1.71	253	1.56×10^{11}
	1.81	258	1.08×10^{11}
	1.91	258	7.53×10^{10}
	2.01	258	5.29×10^{10}
	2.12	262	3.97×10^{10}
	2.37	268	2.46×10^{10}
	2.56	267	1.74×10^{10}
	2.76	266	1.25×10^{10}
	2.98	268	9.70×10^{9}
	3.38	266	5.79×10^{9}
	3.89	267	3.40×10^{9}
97.05.05	1.51	71	5.05×10^{11}
	1.73	81	1.71×10^{11}
	1.95	84	8.45×10^{10}
	2.42	96	3.58×10^{10}
	2.69	93	2.01×10^{10}
	3.21	93	9.47×10^{9}
	3.73	92	5.40×10^{9}

Table 13: CH HI Lyα Intensities at the Solar Minimum (see Figure 7)

Date	Distance ($R_\odot$)	Intensity ($ph\ cm^{-2}\ s^{-1}\ sr^{-1}$)
96.04.06	1.46	1.11×10^{11}
	1.49	8.37×10^{10}
	1.52	6.75×10^{10}
	1.55	5.48×10^{10}
	1.58	4.47×10^{10}
	1.62	3.78×10^{10}
	1.65	3.14×10^{10}
	1.68	2.57×10^{10}
	1.71	2.11×10^{10}
	1.74	1.77×10^{10}
	1.77	1.53×10^{10}
	1.80	1.31×10^{10}
	1.83	1.15×10^{10}
	1.87	9.09×10^{9}
	1.93	6.69×10^{9}
	1.99	5.04×10^{9}
	2.05	4.07×10^{9}
	2.11	3.24×10^{9}
	2.19	2.27×10^{9}
	2.28	1.69×10^{9}
	2.40	1.12×10^{9}
96.05.16	1.51	7.28×10^{10}
	2.01	4.84×10^{9}
	1.76	1.62×10^{10}
	2.26	1.71×10^{9}
96.05.21	1.51	6.34×10^{10}
	1.61	3.53×10^{10}
	1.71	2.00×10^{10}
	1.81	1.25×10^{10}
	1.91	7.69×10^{9}
	2.11	3.38×10^{9}
	2.31	1.48×10^{9}
	2.51	7.87×10^{8}
	2.71	3.90×10^{8}
	3.01	1.77×10^{8}
	3.51	4.15×10^{7}
96.08.29	1.51	1.37×10^{11}
	1.56	9.20×10^{10}
	1.61	6.31×10^{10}
	1.66	4.46×10^{10}
	1.71	3.16×10^{10}
	1.76	2.40×10^{10}
	1.81	1.80×10^{10}
	1.86	1.32×10^{10}
	1.91	1.04×10^{10}
	2.41	1.58×10^{9}
97.05.03	1.61	5.41×10^{10}
	1.81	1.63×10^{10}
	2.01	6.28×10^{9}
	2.31	1.89×10^{9}
	2.71	4.84×10^{8}
97.05.09	1.61	6.01×10^{10}
	1.81	1.70×10^{10}
	2.01	6.22×10^{9}
	2.31	1.72×10^{9}
	2.71	4.36×10^{8}
97.12.20	1.51	4.82×10^{10}
	1.61	2.57×10^{10}
	1.71	1.50×10^{10}
	1.81	8.97×10^{9}
	2.01	3.59×10^{9}
	2.31	1.20×10^{9}
	2.71	3.46×10^{8}
	3.11	1.11×10^{8}
	3.61	4.29×10^{7}
	4.21	3.96×10^{7}
	4.81	3.30×10^{7}
	5.40	2.75×10^{7}

Table 14: Streamer OVI 1032 Intensities at the Solar Minimum (see Figure 14)

Date	Distance ($R_\odot$)	PA (deg)	Intensity ($ph\ cm^{-2}\ s^{-1}\ sr^{-1}$)
96.04.11	1.53	267	1.84×10^{10}
	1.80	268	6.82×10^{9}
	1.98	268	2.57×10^{9}
	2.28	268	1.14×10^{9}
	2.71	268	3.70×10^{8}
	3.15	269	1.89×10^{8}
96.06.04	1.54	84	5.90×10^{10}
	1.78	85	1.66×10^{10}
	2.01	86	5.66×10^{9}
	2.58	80	5.43×10^{8}
	3.13	81	1.83×10^{8}
96.08.31	1.43	253	2.68×10^{10}
	1.55	258	1.73×10^{10}
	1.66	253	9.72×10^{9}
	1.77	258	5.61×10^{9}
	1.89	258	3.99×10^{9}
	2.00	258	3.06×10^{9}
	2.12	262	2.17×10^{9}
	2.34	268	9.57×10^{8}
	2.56	267	5.59×10^{8}
	2.78	266	2.92×10^{8}
	2.00	268	1.58×10^{8}

Table 15: CH OVI 1032 Intensities at the Solar Minimum (see Figure 15)

Date	Distance ($R_\odot$)	Intensity ($ph\ cm^{-2}\ s^{-1}\ sr^{-1}$)
96.04.06	1.36	7.16×10^{9}
	1.38	6.15×10^{9}
	1.40	5.75×10^{9}
	1.42	4.85×10^{9}
	1.43	4.38×10^{9}
	1.45	3.80×10^{9}
	1.47	3.42×10^{9}
	1.49	2.97×10^{9}
	1.51	2.73×10^{9}
	1.52	2.40×10^{9}
	1.54	1.89×10^{9}
	1.56	1.68×10^{9}
96.05.16	1.46	3.47×10^{9}
	2.04	6.00×10^{7}